Phosphoacceptors Threonine 162 and Serines 170 and 178 within the Carboxyl-Terminal RRRS/T Motif of the Hepatitis B Virus Core Protein Make Multiple Contributions to Hepatitis B Virus Replication

Jaesung Jung,[a,b] Seong Gyu Hwang,[c,d] Yong-Joon Chwae,[a,b] Sun Park,[a,b] Ho-Joon Shin,[a,b] Kyongmin Kim[a,b]

Department of Microbiology, Ajou University School of Medicine, Suwon, South Korea[a]; Department of Biomedical Science, Graduate School of Ajou University, Suwon, South Korea[b]; Institute for Clinical Research, CHA Bundang Medical Center, CHA University, Seongnam, South Korea[c]; Department of Internal Medicine, CHA Bundang Medical Center, CHA University, Seongnam, South Korea[d]

ABSTRACT

Phosphorylation of serines 157, 164, and 172 within the carboxyl-terminal SPRRR motif of the hepatitis B virus (HBV) core (C) protein modulates HBV replication at multiple stages. Threonine 162 and serines 170 and 178, located within the carboxyl-terminal conserved RRRS/T motif of HBV C protein, have been proposed to be protein kinase A phosphorylation sites. However, *in vivo* phosphorylation of these residues has never been observed, and their contribution to HBV replication remains unknown. In this study, [^{32}P]orthophosphate labeling of cells expressing C proteins followed by immunoprecipitation with anti-HBc antibody revealed that threonine 162 and serines 170 and 178 are phosphoacceptor residues. A triple-alanine-substituted mutant, mimicking dephosphorylation of all three residues, drastically decreased pregenomic RNA (pgRNA) encapsidation, thereby decreasing HBV DNA synthesis. In contrast, a triple-glutamate-substituted mutant, mimicking phosphorylation of these residues, decreased DNA synthesis without significantly decreasing encapsidation. Neither triple mutant affected C protein expression or core particle assembly. Individual alanine substitution of threonine 162 significantly decreased minus-strand, plus-strand, and relaxed-circular DNA synthesis, demonstrating that this residue plays multiple roles in HBV DNA synthesis. Double-alanine substitution of serines 170 and 178 reduced HBV replication at multiple stages, indicating that these residues also contribute to HBV replication. Thus, in addition to serines 157, 164, and 172, threonine 162 and serines 170 and 178 of HBV C protein are also phosphorylated in cells, and phosphorylation and dephosphorylation of these residues play multiple roles in modulation of HBV replication.

IMPORTANCE

Threonine 162, within the carboxyl-terminal end of the hepatitis B virus (HBV adw) core (C) protein, has long been ignored as a phosphoacceptor, even though it is highly conserved among mammalian hepadnaviruses and in the overlapping consensus RxxS/T, RRxS/T, and TP motifs. Here we show, for the first time, that in addition to the well-known phosphoacceptor serines 157, 164, and 172 in SPRRR motifs, threonine 162 and serines 170 and 178 in the RRRS/T motif are phosphorylated in cells. We also show that, like serines 157, 164, and 172, phosphorylated and dephosphorylated threonine 162 and serines 170 and 178 contribute to multiple steps of HBV replication, including pgRNA encapsidation, minus-strand and plus-strand DNA synthesis, and relaxed-circular DNA synthesis. Of these residues, threonine 162 is the most important. Furthermore, we show that phosphorylation of C protein is required for efficient completion of HBV replication.

Hepatitis B virus (HBV), a prototype hepadnavirus, has a partially double-stranded relaxed-circular (RC) DNA genome that contains four open reading frames (ORFs), encoding the core (C; also called HBc), viral polymerase (P), X (HBx), and surface (S; also called HBs) proteins. HBV replicates by reverse transcription of a pregenomic RNA (pgRNA) within cytoplasmic core particles (often termed the nucleocapsid) composed of viral C proteins (1).

The HBV C protein consists of 183 or 185 amino acids, in the ayw or adw subtype, respectively, although its amino-terminal 149 amino acids are sufficient to direct core particle assembly (2). The carboxyl-terminal 34 (ayw) or 36 (adw) amino acids contain a protamine-like nucleic acid-binding domain rich in arginines that are important for HBV replication (3–6). In addition to the arginine-rich domains, the carboxyl-terminal domain of C protein also contains eight putative phosphorylation sites: seven serines and one threonine (4, 5, 7–11). Among these residues, three serines, at positions 157, 164, and 172 in the adw subtype (positions

155, 162, and 170 in the ayw subtype), each of which is in an SPRRR motif, are phosphorylated *in vitro* by kinases such as the cyclin-dependent protein kinase p34^{cdc2} (also known as CDK1) (12), Ca^{2+}- and phospholipid-dependent protein kinase (PKC) (13), the 46-kDa serine protein kinase (14), serine/arginine-rich protein kinases 1 and 2 (SRPK1/2) (15), and cyclin-dependent protein kinase 2 (CDK2) (16). Using double-, triple-, and quintuple-alanine-substituted mutants, Daub et al. (15) indirectly showed that serines 178 and 180 (adw) are phosphorylated in cells,

although they did not analyze these residues individually. All seven serines (serines 157, 164, 170, 172, 178, 180, and 183 in the adw subtype) have been suggested to be potential SRPK phosphorylation sites (17). SRPK1 and SRPK2 have relaxed consensus recognition sites but cannot phosphorylate threonine. Enomoto and colleagues demonstrated that serines 170 and 178 are phosphorylated by casein kinase 2 (CK2)-activated protein kinase A (PKA) *in vitro*, and they further suggested that threonine 162 and serines 170 and 178, in the conserved RRxS/T motif, may be the phosphoacceptor sites for PKA (18). Serines 87 and 106 in the carboxyl-terminally truncated genotype C of HBV C protein are phosphorylated *in vitro* by PKA and PKC, respectively, and these modifications facilitate capsid assembly and stability (19, 20). In contrast, the HBV adw and adw2 subtypes have asparagine and serine at positions 87 and 106, respectively.

Among the kinases mentioned above, PKC, the 46-kDa serine protein kinase, and CDK2 associate with the core particle (13, 14, 16). Kann and Gerlich (13) also showed that PKA binds the carboxyl terminus of C protein during core particle assembly and is encapsidated by reconstituted core particles, although the binding affinity and encapsidation efficiency of PKA are lower than those of PKC. However, it is possible that neither PKA nor PKC is responsible for phosphorylation of the carboxyl terminus of C protein and its incorporation into core particles (14, 15). Although the identities of the core particle-associated kinases that are responsible for phosphorylation of C protein remain controversial, recent work has shown that CDK2 or a CDK2-like kinase, the proline-directed serine/threonine kinase, is incorporated into core particles and can phosphorylate hepadnavirus C protein at S/TP sites (16).

The conserved phosphoacceptor serines 157, 164, and 172 in the SPRRR motif are important for core particle formation, RNA packaging (7, 11, 13, 21), DNA synthesis (4, 7, 11, 22, 23), and subcellular localization (24, 25). Threonine 162 and serines 170 and 178 in the RRRS/T motif are also conserved among mammalian hepadnaviruses (Fig. 1), suggesting that these residues contribute to the HBV life cycle. However, it remains unclear whether threonine 162 and serines 170 and 178 are phosphorylated in cells and, if so, whether such modifications contribute to HBV replication. In this study, we found that threonine 162 and serines 170 and 178 serve as phosphoacceptor sites, indicating that C protein can be heavily phosphorylated at up to seven sites (six serines and one threonine). Furthermore, we showed that phosphorylation and dephosphorylation of these three residues contribute in multiple ways to HBV replication. Most importantly, we showed that threonine 162, in the conserved RRRT (RRxT and RxxT) and TP motifs, which was long ignored in this regard, is indeed a phosphoacceptor site that is important for HBV replication.

MATERIALS AND METHODS

DNA construction. To express HBV under the control of the cytomegalovirus immediate early promoter, partially redundant HBV wild-type (WT) subtype adw R9 was subcloned into pcDNA3.1 (Invitrogen); the resultant construct was designated pPB (26). The polymerase (P) protein-deficient mutant, which expresses HBV pgRNA and the HBV C, S, and X proteins, but not P protein, was described previously (26). In this study, this mutant is designated STSSSS (WT) to indicate that it produces the WT HBV C protein. From the P-deficient mutant background, single, double, triple, quintuple, and sextuple phosphorylation site mutants of HBV C protein were generated by PCR-mediated mutagenesis. The resultant mutants were designated the following: the T162A, T162E, S170A,

FIG 1 Sequence alignments of the carboxyl terminus of HBV and those of related hepadnavirus C proteins. Carboxyl-terminal amino acid sequences of C proteins of human HBV (adwR9 subtype), chimpanzee HBV (ChHBV) (accession no. ACY72695.1), orangutan HBV (OrHBV) (accession no. ABY25960.1), ground squirrel hepatitis virus (GSHV) (accession no. AAA46755.1), woodchuck hepatitis virus (WHV) (accession no. AAA46761.1), woolly monkey HBV (WMHBV) (accession no. AAO74859.1), duck hepatitis B virus (DHBV) (accession no. ACA42586.1), heron hepatitis B virus (HHBV) (accession no. AAA45737.1), Ross goose HBV (RGHBV) (accession no. AAA45747.1), snow goose HBV (SGHBV) (accession no. YP_031694.1), and stork HBV (SHBV) (accession no. CAC80812.1) were aligned. Putative SPRRR and RRRS/T phosphorylation sites of HBV are marked with closed and open arrowheads, respectively. Residues shown in bold are putative phosphorylation sites, and underlined and italicized residues are putative phosphorylation sites at conserved RRRS/T motifs.

S170E, S178A, S178E, SSSSSS, T162A/S170A, T162E/S170E, T162A/S178A, T162E/S178E, S170A/S178A, S170E/S178E, 3A-PRRR (ATASAS), 3E-PRRR (ETESES), RRR-3A (SASASA), RRR-3E (SESESE), ATAAAA, AAASAA, AAAAAS, ASAAAA, ETEEEE, ESEEEE, AAAAAA, and EEEEEE mutants. Triple-alanine- and triple-glutamate-substituted mutants of SPRRR motifs were designated 3A-PRRR and 3E-PRRR, respectively. Triple-alanine- and triple-glutamate-substituted mutants of RRRS/T motifs were designated RRR-3A and RRR-3E, respectively. To supply the HBV P protein in *trans*, the HBV-pol-ΔPS construct was used. This construct is an HBV P protein supplier containing a deletion of the 5′-end encapsidation signal and most of the C protein ORF, as well as a mutation in the conserved splice acceptor site at nucleotide (nt) 2941; these mutations were described previously (27). To generate the RT-YMHA-pol-ΔPS mutant construct, the EcoRI- and EcoRV-digested DNA fragment from a reverse transcriptase (RT)-deficient RT-YMHA mutant, wherein the conserved YMDD motif of the RT active site is modified to YMHA (26), was cloned into the HBV-pol-ΔPS construct. All constructs were sequenced to confirm the presence of the introduced mutations and the absence of extraneous mutations.

Cell culture, transfection, core particle isolation, and core particle Western blotting. Huh7 hepatoma cells were grown in Dulbecco's modified Eagle's medium (DMEM) supplemented with 10% fetal bovine serum (FBS; Gibco-BRL) and 1% penicillin-streptomycin under a humidified atmosphere at 37°C in 5% CO_2. Cells were passaged every third day. Huh7 cells were cotransfected into 10-cm dishes by use of polyethylenimine (Polysciences). For cotransfections, 5 μg of P protein-expressing plasmid was mixed with 5 μg of plasmid encoding HBV STSSSS (WT) or phosphoacceptor site mutant C proteins in a P-deficient mutant backbone. As a transfection control, 1 μg of green fluorescent protein (GFP)-expressing plasmid was included in the transfection mixture. Transfection experiments were repeated at least three times. Cytoplasmic core particles were prepared as previously described (26). Isolated core particles were electrophoresed in 1% native agarose gels, and the resolved proteins were transferred to polyvinylidene fluoride (PVDF) membranes (Millipore). Immunoblotting to visualize core particles was performed using polyclonal rabbit anti-HBc primary antibody (1:1,000 dilution) (3) and horseradish peroxidase-conjugated anti-rabbit secondary antibody (1:2,000 di-

lution) (Dako). Bound secondary antibodies were visualized by enhanced chemiluminescence (ECL Western blotting detection reagent; Amersham). The relative intensities of core particles were measured using Fujifilm Image Gauge software, version 4.0.

SDS-PAGE and Western blotting. Equal quantities of protein from whole-cell lysates (0.1% Triton X-100, 0.5% sodium deoxycholate, and 0.1% SDS) containing 1 mM phenylmethylsulfonyl fluoride were subjected to sodium dodecyl sulfate-polyacrylamide gel electrophoresis (SDS-PAGE) on 12% gels, transferred to PVDF membranes, and then incubated with the appropriate primary antibodies (polyclonal rabbit anti-HBc [1:1,000] and polyclonal rabbit anti-GFP [1:1,000] [Santa Cruz Biotechnology]), followed by anti-rabbit secondary antibodies coupled to horseradish peroxidase (1:2,000 dilution) (Dako). The blots were then visualized by ECL. The relative intensities were measured using Fujifilm Image Gauge software, version 4.0. Transfection efficiencies were normalized and compared by Western blotting of GFP.

Phosphorylation of HBV C proteins in the cell. Forty-eight hours after transfection, Huh7 cells were incubated for 6 h in DMEM containing 10% dialyzed FBS, labeled for 14 h with 250 μCi [^{32}P]orthophosphate ($^{32}P_i$) (New England Nuclear) per 10^7 cells, rinsed with ice-cold phosphate-buffered saline, and lysed with 1 ml of lysis buffer (50 mM Tris-HCl [pH 8.5], 2 mM EDTA, 0.5% Nonidet P-40, 50 mM NaF, 25 mM β-glycerophosphate, 2 mM sodium orthovanadate, and protease inhibitors). The lysates were incubated for 2 h at 4°C with 1 μl of polyclonal rabbit anti-HBc antibody. Next, 15 μl of protein A/G Plus agarose beads (Abcam) was added, and the mixture was incubated at 4°C for 1 h and centrifuged. The pellets (containing beads bound to immune complexes of radiolabeled WT or mutant C proteins and anti-HBc antibodies) were washed twice with lysis buffer, eluted by boiling in 2× sample buffer (100 mM Tris-HCl [pH 6.8], 4% SDS, 200 mM β-mercaptoethanol, 0.2% bromophenol blue, and 20% glycerol), and separated by SDS-PAGE on 13.5% gels. Separated proteins were transferred to PVDF membranes and subjected to autoradiography.

Southern blotting. To analyze HBV DNA synthesis by Southern blotting, HBV DNAs extracted from isolated core particles were separated by agarose gel electrophoresis, transferred to nylon membranes, and hybridized to a ^{32}P-labeled random-primed probe specific for the HBV sequence, as described previously (26). Relative intensities were measured using Fujifilm Image Gauge software, version 4.0. For Fig. 4C, HBV DNAs extracted from isolated core particles were heat denatured at 100°C for 5 min, immediately cooled on ice, and then separated by agarose gel electrophoresis.

RPA. For analysis of cytoplasmic and encapsidated pgRNAs, RNase protection analysis (RPA) was performed as previously described (26). Encapsidated pgRNAs were extracted from core particles isolated from cotransfected Huh7 cells grown in 10-cm dishes and then electrophoresed in a 5% polyacrylamide–8 M urea gel. For analysis of cytoplasmic pgRNAs, total RNA was extracted using RNA-STAT-60 (Tel-Test, Inc.), and 5 μg of total RNA was electrophoresed. The 446- and 470-nt radiolabeled antisense RNA probes were synthesized *in vitro*. The protected pgRNAs were 369 and 413 nt, corresponding to nt 1819 to 2187 and 1262 to 1674 of the HBV sequence, respectively (3, 26, 27). The relative levels of pgRNAs were measured using Fujifilm Image Gauge software, version 4.0.

EPA. Isolated core particles were incubated overnight at 37°C in endogenous polymerase assay (EPA) reaction buffer (50 mM Tris-HCl [pH 7.5], 75 mM NH$_4$Cl, 1 mM EDTA, 25 mM MgCl$_2$, 0.1% β-mercaptoethanol, and 0.5% Nonidet P-40) supplemented with a 0.5 mM concentration (each) of dCTP, dGTP, and TTP and 10 μCi [α-^{32}P]dATP (26). ^{32}P-labeled DNA was extracted after the EPA reaction, separated in a 1% agarose gel, and then subjected to dry-gel autoradiography (26).

Nucleic acid blotting. To detect nucleic acids *in situ* from core particles formed by WT and mutant C proteins, micrococcal nuclease-digested cell lysates were subjected to 1% native agarose gel electrophoresis and then transferred to PVDF membranes. Membranes were denatured with 0.2 N NaOH and 150 mM NaCl for 1 min, neutralized with 100 mM

Tris-HCl (pH 7.2), and soaked in 20× saline-sodium citrate buffer (3 M NaCl, 0.3 M sodium citrate [pH 7.0]) for 1 min, and then nucleic acids on the membrane were cross-linked by UV irradiation. Hybridization was performed as described above for Southern blotting.

Primer extension analysis. Oligonucleotide DNA primers were 5′ end labeled with 30 μCi [γ-^{32}P]ATP at 37°C for 3 h by use of T4 polynucleotide kinase. The 5′-end-labeled primers HBV1665+ (5′-CTCTTGG ACTCTCAGCAATGTCAAC-3′), HBV1744− (5′-CAGCTCCTCCCAG TCCTTAAACA-3′), and HBV1952− (5′-GAGAGTAACTCCACAGTAG CTCC-3′) were used to measure the levels of the elongated minus-strand, plus-strand, and RC DNAs, respectively. HBV DNA extracted from core particles isolated from cotransfected Huh7 cells in 10-cm dishes was divided into four batches: one batch for Southern blotting and three batches for primer extensions to measure minus-strand, plus-strand, and RC DNAs. For primer extension analyses of each C protein variant, 1 ng of internal standard (IS) DNA was added to each viral DNA-containing reaction mixture [20 mM Tris-HCl (pH 8.8), 10 mM (NH$_4$)$_2$SO$_4$, 10 mM KCl, 10 mM MgSO$_4$, and 0.1% Triton X-100] supplemented with a 2 mM concentration of each deoxynucleoside triphosphate (dNTP). The mixtures were heated to 95°C for 5 min, treated with 1 U RNase A at 37°C for 1 h, ethanol precipitated, and resuspended in distilled water. End-labeled primers were extended with Vent Exo (−) polymerase (New England BioLabs), yielding products that annealed to the respective complementary HBV DNA sequences. The extended products were electrophoresed through 5% polyacrylamide gels containing 8 M urea. Dried gels were subjected to autoradiography, and relative levels were measured using Fujifilm Image Gauge software, version 4.0.

Immunoprecipitation, SDS-PAGE, and Western blotting. Huh7 cells were cotransfected as described in "Cell culture, transfection, core particle isolation, and core particle Western blotting." Three days after cotransfection, cells were lysed with 1 ml of lysis buffer as described in "Phosphorylation of HBV C proteins in the cell." Cell debris was removed by centrifugation at 13,000 rpm at 4°C for 2 min. The supernatant was collected and incubated for 2 h at 4°C with 1 μl of polyclonal rabbit anti-HBc antibody, after which 15 μl of protein A/G Plus agarose beads was added. The beads, bound to immune complexes consisting of anti-HBc antibodies and WT or mutant C proteins, were pelleted by centrifugation and washed twice with lysis buffer. Bound proteins were eluted by boiling in 2× SDS-PAGE sample buffer, separated by SDS-PAGE on 13.5% gels, and subjected to Western blotting as described in "SDS-PAGE and Western blotting."

RESULTS

Carboxyl-terminal amino acid sequence alignments reveal putative phosphoacceptor sites in hepadnaviral C proteins. To begin our analysis, we generated amino acid sequence alignments of the carboxyl termini of hepadnaviral C proteins. These alignments revealed that the well-studied serine phosphoacceptors in the SPRRR motifs (Fig. 1, closed arrowheads) and the putative phosphoacceptors in the RRRS/T (or RRxS/T) motifs (Fig. 1, open arrowheads) are highly conserved among mammalian hepadnaviruses but not among avian hepadnaviruses (Fig. 1, compare upper and lower alignments). While scrutinizing the carboxyl-terminal consensus phosphorylation motifs, we noticed that among the seven serines and one threonine, all but one (serine 183) appear in the context of RxxS/T phosphoacceptor motifs, which also overlap other consensus motifs. Three of the serines and the threonine are present in conserved putative phosphoacceptor S/TP motifs, and three of the serines are in RS motifs (Fig. 1). In the most divergent primate hepadnavirus, woolly monkey HBV (WMHBV), the conservation is somewhat relaxed.

The motif contexts of three of these putative phosphoacceptor residues (for threonine 162, RRRT [or RRxT], RxxT, and TP; and for serines 170 and 178, RRRS [or RRxS], RxxS, and RS) suggest
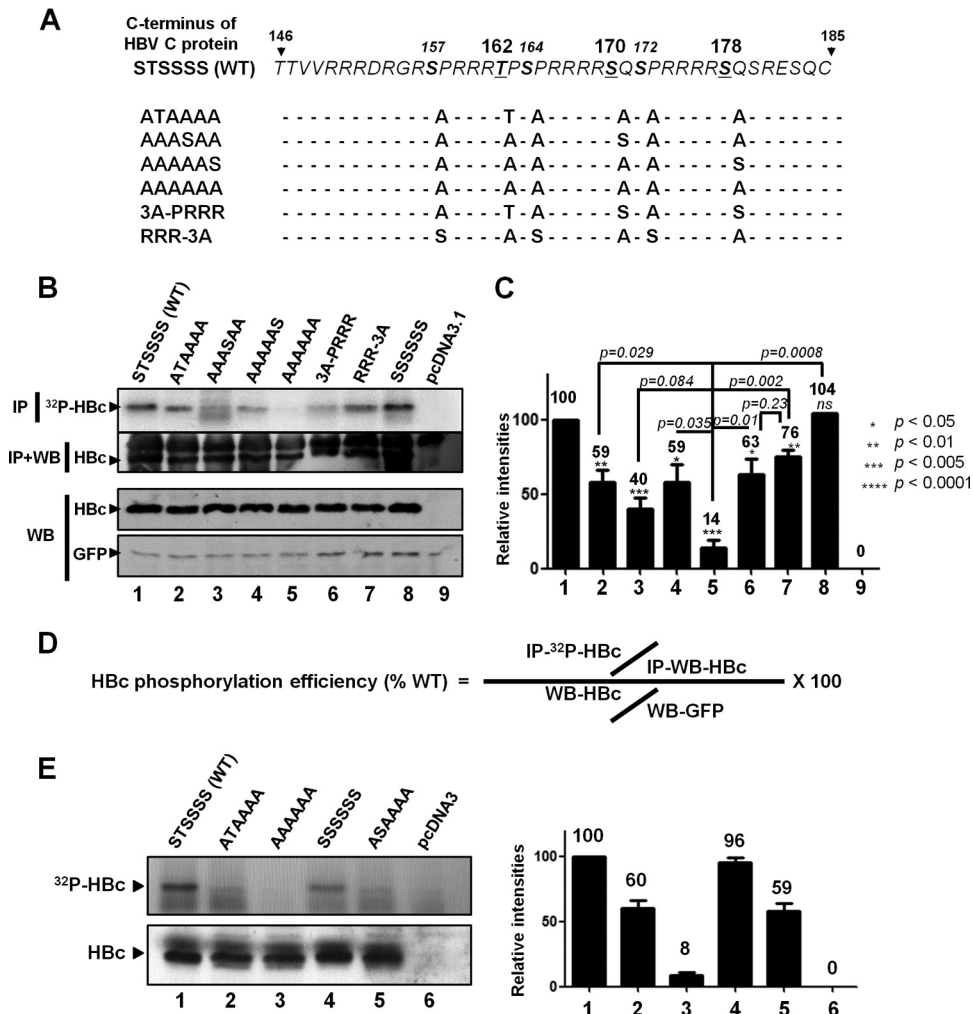
FIG 2 Phosphorylation of threonine 162 and serines 170 and 178 of HBV mutant C proteins in cells. (A) Carboxyl-terminal sequences of WT and alanine-substituted mutant C proteins. (B) Phosphorylation of WT and mutant C proteins in cells. Huh7 cells were transfected with constructs encoding the STSSSS (WT), ATAAAA, AAASAA, AAAAAS, AAAAAA, RRR-3A, 3A-PRRR, and SSSSSS mutants or with pcDNA3. Two days after transfection, the cells were labeled with [^{32}P]orthophosphate, immunoprecipitated (IP) with anti-HBc antibody, and subjected to SDS-PAGE and autoradiography (top panel). Labeled and immunoprecipitated C proteins were also determined by Western blotting (WB) (second panel). Western blotting was performed to check the expression of C protein (third panel). To normalize the labeling intensities, a cotransfected GFP (bottom panel) construct was used as a control for loading and transfection efficiency. GFP was detected by Western blotting. (C) Relative intensities of phosphorylated STSSSS (WT) and mutant C proteins. Data represent means and standard deviations (SD) of results from three independent experiments. The statistical significance of differences was evaluated using Student's t test. P values for differences relative to the STSSSS (WT) protein are indicated by asterisks: *, $P < 0.05$; **, $P < 0.01$; ***, $P < 0.005$; and ****, $P < 0.0001$. P values for differences relative to the AAAAAA mutant are shown above the bars. (D) Equations used to calculate the phosphorylation efficiencies of WT and mutant C proteins. The autoradiographic intensity of ^{32}P$_i$-labeled C protein normalized against the protein level detected by immunoprecipitation and Western blotting was divided by the level of C protein detected by Western blotting normalized against the transfection efficiency (as determined from GFP expression). (E) Phosphorylation of additional mutant C proteins in cells. ^{32}P$_i$-labeled lysates of Huh7 cells expressing the STSSSS (WT), ATAAAA, AAAAAA, SSSSSS, and ASAAAA mutants or pcDNA3 were prepared as described for panel B.

that various cellular kinases phosphorylate these residues. Based on prior observations that phosphoacceptor serines 157, 164, and 172 (adw subtype) modulate HBV replication at multiple steps ([4], [7], [11], [21]–[25]), we hypothesized that phosphorylation and dephosphorylation of threonine 162 and serines 170 and 178 may also contribute to HBV replication.

Threonine 162 and serines 170 and 178 of hepadnaviral C proteins are phosphoacceptor sites. To determine whether threonine 162 and serines 170 and 178 are indeed phosphoacceptor residues in cells, we constructed a series of C-protein-expressing mutants in a P-protein-deficient background. In these experi-

ments, the version of the protein containing all six putative phosphoacceptor residues (S157, T162, S164, S170, S172, and S178) is referred to as the STSSSS (WT) protein. In the AAAAAA mutant, all six of these residues were replaced with alanines, abolishing the putative phosphoacceptor sites ([Fig. 2A]). Two triple-alanine-substituted alleles were also generated: 3A-PRRR, in which the putative phosphoacceptors in SPRRR motifs were replaced (S157A, S164A, and S172A [ATASAS]); and RRR-3A, in which the putative phosphoacceptors in RRRS/T motifs were replaced (T162A, S170A, and S178A [SASASA]) ([Fig. 2A]). To precisely define the phosphoacceptor residue(s), threonine 162, serine 170, and serine

178 were each singly restored in the AAAAAA mutant background, yielding the ATAAAA, AAASAA, and AAAAAS mutants, respectively (Fig. 2A). Huh7 cells transfected with each variant were labeled with ^{32}P$_i$ for 14 h and then lysed. The ^{32}P$_i$-labeled lysates were immunoprecipitated with anti-HBc antibody, and the ^{32}P$_i$-labeled immunoprecipitated C proteins were detected by autoradiography (Fig. 2B, top panel). Immunoprecipitation followed by Western blotting revealed that the anti-HBc antibody could recognize all of the variant proteins (Fig. 2B, second panel), and Western blotting of lysates revealed that all mutant C proteins were expressed at comparable levels (Fig. 2B, third panel). The efficiency of phosphorylation in cells transfected with either STSSSS (WT) or mutant C protein was calculated according to the equation shown in Fig. 2D. This calculation was performed on samples from cells transfected with either STSSSS (WT) or mutant C protein. Therefore, a weak labeling intensity was not due to low levels of expression, inability of the anti-HBc antibody to recognize the mutant C proteins, or instability of the mutant C proteins (Fig. 2B, top three panels). The ^{32}P$_i$-labeled C protein from STSSSS (WT) protein-transfected cells was clearly detectable (Fig. 2B, top panel, lane 1). In contrast, the AAAAAA mutant exhibited extremely weak labeling (Fig. 2B, top panel, and C, lanes 5) that was comparable to that of pcDNA-transfected cells, used as a negative control (Fig. 2B, top panel, and C, lanes 9), suggesting that serines 180 and 183 and the amino-terminal serines are phosphorylated weakly, if at all. Although these residues have not been examined individually, a previous study showed that serine 178 and/or 180 is phosphorylated *in vivo* (15). The labeling intensity of the 3A-PRRR mutant was slightly but not significantly weaker than that of the RRR-3A mutant (Fig. 2B, top panel, and C, compare lanes 6 and 7). Although threonine 162, serine 170, and serine 178 could be phosphorylated individually, serine 170 was a weaker phosphoacceptor (Fig. 2B, top panel, and C, lanes 1 versus lanes 2, 3, and 4 versus lanes 5). When only one phosphoacceptor site was available, as in the ATAAAA, AAASAA, and AAAAAS mutants, phosphorylation was quite efficient, with labeling intensities of 40 to 59% of that of the STSSSS (WT) protein (Fig. 2B, top panel, and C, lanes 1 versus lanes 2 to 4). Nevertheless, the labeling intensities of WT and mutant C proteins demonstrated that none of the six phosphoacceptor sites, including the three newly identified sites in this study, is always phosphorylated at any given time.

When threonine 162 was replaced by serine (SSSSSS), labeling was comparable to that of the STSSSS (WT) protein (Fig. 2B, top panel, and C, lanes 1 versus lanes 8, and Fig. 2E, left panels, lane 1 versus lane 4). The labeling intensities of the ATAAAA and ASAAAA mutants were also comparable (Fig. 2E, left panels, lane 2 versus lane 5). Taken together with previous observations (13–16), our results demonstrate that the carboxyl terminus of the HBV C protein has at least seven phosphoacceptor sites (serines 157, 164, 170, 172, 178, and 180 and threonine 162) that can be recognized and phosphorylated by various cellular kinases.

Core particle assembly by phosphorylation site mutant C proteins. Based on the phosphorylation of threonine 162 and serines 170 and 178 in conserved RRRS/T motifs (Fig. 2B and E), we investigated whether phosphorylation and/or dephosphorylation of these residues could modulate HBV replication, as in the case of serines 157, 164, and 172 in the SPRRR motifs (7, 11, 13, 14, 21, 22, 25). To address this issue, we constructed additional C-protein mutants in the P-deficient mutant background by replacing threonine and serines with glutamates (Fig. 3A, bottom panel). All of

the mutant C proteins were expressed at comparable levels in transfected Huh7 cells (Fig. 3B, top panel). Native agarose gel electrophoresis followed by Western blotting revealed that core particles formed by mutant C proteins exhibited slightly different migration patterns (Fig. 3B, second panel, lanes 2 to 8), as previously reported for other mutant C proteins (3). When core particle assembly and C protein expression were measured and normalized to pGFP transfection efficiencies, no significant differences were observed (Fig. 3C and D).

Impaired HBV DNA synthesis and absence of RC DNA in the presence of mutant C proteins. To investigate the effects of phosphorylation and/or dephosphorylation of threonine 162 and serines 170 and 178 on HBV replication, we analyzed HBV DNA synthesis by Southern blotting of Huh7 cells cotransfected with HBV-pol-ΔPS and a construct encoding the STSSSS (WT), 3A-PRRR, 3E-PRRR, RRR-3A, RRR-3E, AAAAAA, or EEEEEE protein. RC DNA was easily detectable in cells expressing the STSSSS (WT) protein (Fig. 4A and B, lanes 1) but not in cells expressing any of the mutants (Fig. 4A and B, lanes 2 to 7). A previous report showed that the alanine-substituted 3A-PRRR mutant causes more dramatic defects in HBV DNA synthesis than the glutamate-substituted 3E-PRRR mutant (11). Consistent with these observations, the RRR-3A and AAAAAA mutants caused more dramatic defects than the RRR-3E and EEEEEE mutants, respectively (Fig. 4A and B, lanes 2, 4, and 6 versus lanes 3, 5, and 7, respectively). DNAs smaller than double-stranded linear (DL) DNA were more prominent in cells expressing glutamate-substituted mutants than in those expressing alanine-substituted mutants (Fig. 4A, asterisks, lanes 3, 5, and 7 versus lanes 2, 4, and 6, respectively). To characterize the DNAs smaller than DL and single-stranded minus-sense HBV (SS) DNAs, we heat denatured HBV DNA prior to gel electrophoresis. As expected, RC DNA disappeared from cells cotransfected with the STSSSS (WT) protein (Fig. 4C, lane 1), whereas the levels of SS DNA rose dramatically in cells cotransfected with STSSSS (WT) or mutant protein (Fig. 4C, lanes 1 to 5 and 7), with the exception of the AAAAAA mutant, which was too defective to be recognized (Fig. 4C). SS DNAs were more abundant in cells expressing the 3E-PRRR and RRR-3E mutants than in those expressing the STSSSS (WT) protein (Fig. 4C, lane 1 versus lanes 3 and 5), indicating that the defect was not in minus-strand DNA synthesis but, instead, in the following steps. Unexpectedly, however, we still detected DNA comparable in size to DL DNA with the STSSSS (WT) or mutant protein, with the exception of the AAAAAA and EEEEEE mutants (Fig. 4C). The presence of DL DNA after heat denaturation was reported in a previous study, prompting the authors to speculate that rapid renaturation might occur either following denaturation or during gel electrophoresis (28). When we heat denatured 100 pg of a 3.2-kbp FspI-digested HBV DNA monomer, we were able to detect SS DNA as a faint band (data not shown), supporting the rapid-renaturation hypothesis. To confirm the results of Southern blotting, we also performed an EPA, which yielded a result similar to that shown in Fig. 4A (data not shown). These data provide the first demonstration that phosphorylation and dephosphorylation of threonine 162 and serines 170 and 178 may be important for HBV replication.

Triple-alanine-substituted mutant HBV C proteins are defective in pgRNA encapsidation. To determine whether the reduction in HBV DNA synthesis in cells expressing phosphoacceptor site mutants was due to inefficient pgRNA encapsidation (7, 11), we cotransfected Huh7 cells with RT-YMHA-pol-ΔPS and a
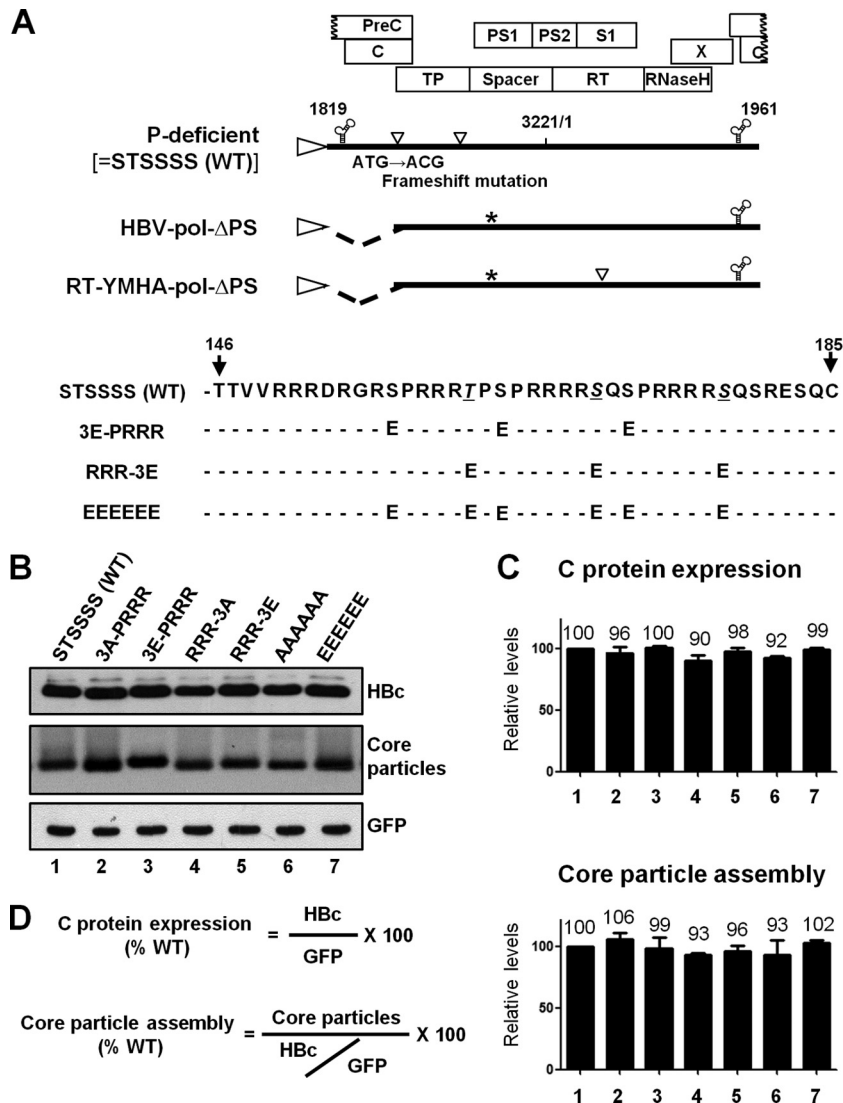
FIG 3 Core particle assembly by STSSSS (WT) and mutant C constructs. (A) (Top) Schematic diagrams of P-deficient strain (here designated the STSSSS [WT] strain because the C protein is WT), HBV-pol-ΔPS, and RT-YMHA-pol-ΔPS. The positions of point mutations are indicated as open arrowheads. Four ORFs are shown at the top, as open boxes. HBV-pol-ΔPS produces WT P protein with a mutation at the splice acceptor site (asterisk). The P protein from RT-YMHA-pol-ΔPS, with the splice acceptor site mutation (asterisk), is RT deficient but encapsidates pgRNA. (Bottom) Positions of substituted residues in glutamate-substituted triple- and sextuple-mutant C proteins. (B) C proteins and core particles produced by STSSSS (WT) and mutant C constructs. Lysates from Huh7 cells transfected with the STSSSS (WT) and mutant C proteins were subjected to SDS-PAGE (13.5% gels) and Western blotting using polyclonal rabbit anti-HBc antibody (top panel). To detect core particles formed by STSSSS (WT) and mutant C proteins, isolated core particles were subjected to native agarose gel electrophoresis, transferred to PVDF membranes, and incubated with polyclonal rabbit anti-HBc antibody (second panel). GFP (bottom panel), used as a loading and transfection control, was detected by Western blotting. (C) Relative levels of C protein expression and core particle assembly by STSSSS (WT) and mutant C constructs. Data represent the means and SD of results from three independent experiments. Statistical significance was evaluated using Student's *t* test. (D) Equations to calculate C protein expression and the amount of core particle assembly. C protein expression was normalized to transfection efficiency (as determined from GFP expression), and core particle assembly was normalized to C protein expression.

plasmid encoding the STSSSS (WT), 3A-PRRR, 3E-PRRR, RRR-3A, RRR-3E, AAAAAA, or EEEEEE protein. The RT-deficient, P-protein-expressing plasmid RT-YMHA-pol-ΔPS was used as a supplier of P protein to allow measurement of pgRNA encapsidation alone, i.e., excluding the effect of HBV DNA synthesis. Intracellular RNAs and RNAs extracted from core particles were analyzed by an RNase protection assay (RPA) (Fig. 5A and B). Intracellular pgRNAs were all expressed at comparable levels (Fig. 5A, second panel). In the glutamate-substituted mutants, pgRNA encapsidation was extremely efficient compared to DNA synthesis

(Fig. 4B versus 5B, lanes 3, 5, and 7). Consistent with a previous report (7, 11, 22), pgRNA encapsidation was severely impaired in the alanine-substituted mutants (Fig. 5A, top panel), comparable to the results of Southern blotting (Fig. 4), demonstrating that the defects in HBV DNA synthesis in the alanine-substituted mutants were due to impaired encapsidation. Therefore, as in the case of phosphorylated serines 157, 164, and 172, previously shown to contribute to pgRNA encapsidation (7, 11, 22), phosphorylated threonine 162 and serines 170 and 178 also contribute to encapsidation.

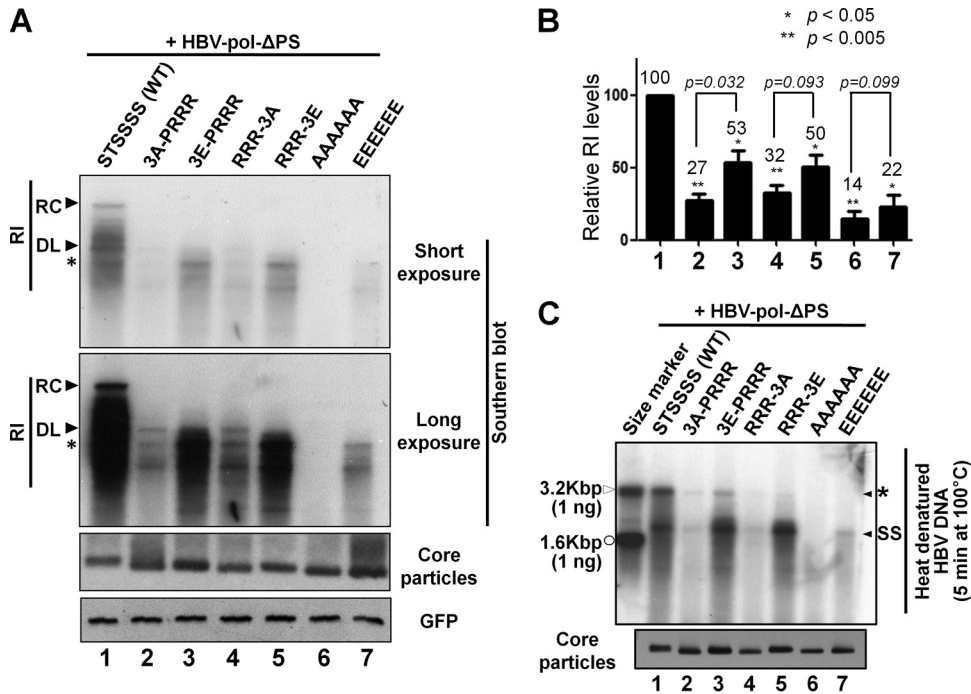An RPA probe specific to the 5′ end of pgRNA can bind to both

FIG 4 HBV DNA synthesis in core particles formed by STSSSS (WT) and mutant C proteins. (A) To examine HBV DNA synthesis in core particles formed by mutant C proteins, HBV-pol-ΔPS and the STSSSS (WT) protein or the indicated mutant C proteins were cotransfected into Huh7 cells. HBV DNA was extracted from isolated core particles, and Southern blot analysis was performed. Core particle formation (third panel) was determined as described in the legend to Fig. 3B. GFP was included as a transfection control (bottom panel), as described in the legend to Fig. 2B. (B) Quantitation of relative levels of HBV DNA from isolated core particles, compared after normalization to transfection efficiency (as determined from GFP expression). Total amounts of replicative-intermediate (RI) DNAs, including RC and DL DNAs, are indicated. Data represent means and SD of results from three independent experiments. Statistical significance was evaluated using Student's t test. P values for differences relative to the STSSSS (WT) protein are indicated by asterisks: *, $P < 0.05$; and **, $P < 0.005$. Comparisons between the alanine- and glutamate-substituted mutants are indicated by brackets, and the P values are shown above the bars. (C) Effect of heat denaturation of HBV DNA. HBV DNAs extracted from cotransfected Huh7 cells as described above were heat denatured at 100°C for 5 min before agarose gel electrophoresis. On the right side, the band comparable in size to DL DNA is marked with an asterisk, and the band comparable in size to SS DNA is marked "SS" (closed arrowheads). The size marker on the left (1 ng of ~3.2-kbp HBV DNA; open arrowhead) was PCR amplified from pPB (26) by using forward primer 273 (5′-GTGGCTTTGGGGCATGGACATTG-3′) and reverse primer 19 (5′-GTGCGCAGACCAATTTATGC-3′). The other size marker (1 ng of ~1.6-kbp HBV DNA; open circle) was the BspEI/XcmI-digested fragment of pPB (26).

full-length and spliced pgRNAs; therefore, the use of a 5′-end probe may cause bias toward encapsidation of full-length pgRNA. Taking into account the results obtained with the 5′-end probe (Fig. 5A), we speculated that the small DNAs detected by Southern blotting (Fig. 4A) might have been synthesized from spliced RNAs (3, 5, 21). To examine the small DNAs, we performed PCR on core particles isolated from cotransfected Huh7 cells. In addition to the full-length DNA, the small DNA was amplified as a major band; sequence analysis revealed that this small DNA represented a 1,257-nt deletion, spanning nt 2455 to 2491, a region which contains one of the most frequently spliced sites (Fig. 5C). When we performed RPA with an internal pgRNA-specific probe to exclude encapsidation of spliced RNA (see Fig. 6C), we did not observe results significantly different from those obtained with the 5′-end probe (data not shown), indicating that there was no significant bias between encapsidation of full-length and spliced RNAs.

Double-mutant HBV C proteins containing the T162A mutation are deficient in pgRNA encapsidation. To investigate the individual roles of threonine 162 and serines 170 and 178 in HBV replication, we constructed additional mutants in which these residues were replaced with alanine or glutamine, either singly or pairwise (Fig. 6A). Levels of C protein expression and core particle assembly were comparable in cells expressing all of these mutants

(Fig. 6B, top and middle panels). Nucleic acid blotting to detect both RNAs and DNAs inside core particles revealed a significant reduction in nucleic acids in core particles from Huh7 cells expressing the T162A, T162A/S170A, T162A/S178A, RRR-3A, and RRR-3E mutants (Fig. 6B, bottom panel), suggesting that these mutants cause defects in HBV replication.

To determine whether the reduction in nucleic acids was due to the low level of pgRNA encapsidation as seen in cells expressing the RRR-3A mutant (Fig. 5A and B, lanes 4), we performed RPA (Fig. 6C, first, second, and third panels). As in Fig. 5A, intracellular RNA levels were comparable in all samples (Fig. 6C, third panel). Consistent with the data in Fig. 5A and B, lanes 4, encapsidation was severely impaired in the RRR-3A mutant (Fig. 6C, first and second panels, lanes 14). Both the 5′-end and internal region probes were used to exclude bias toward encapsidation of full-length or spliced pgRNA (Fig. 6C, compare first and second panels) (27). If spliced RNAs were more abundant or encapsidated more efficiently than full-length pgRNA, the internal region probe would detect less protected RNA than the 5′-end-specific probe. The amounts of encapsidation of full-length and spliced pgRNAs by the T162A/S170A (53% and 39%, respectively) and T162A/S178A (64% and 53%, respectively) mutants were significantly smaller than those by the STSSSS (WT) protein (Fig. 6C,
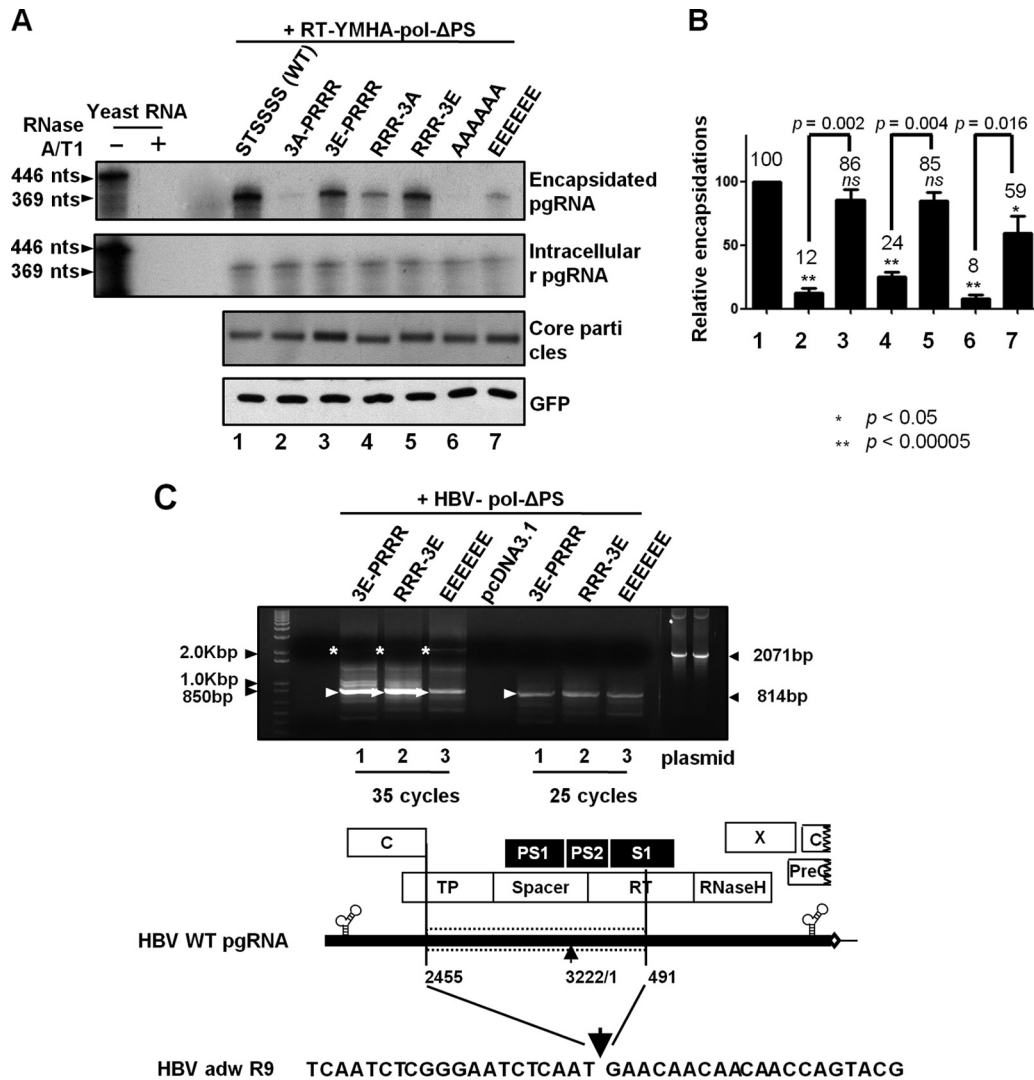
FIG 5 pgRNA encapsidation in core particles formed by STSSSS (WT) and mutant C proteins. (A) RPA to detect HBV intracellular pgRNA and encapsidated pgRNA. An *in vitro*-transcribed radiolabeled antisense RNA probe (446 nt) was hybridized overnight at 50°C with pgRNA from isolated core particles. Following RNase digestion, the protected pgRNA (369 nt), representing nt 1819 to 2187 of the HBV sequence, was electrophoresed in a 5% polyacrylamide–8 M urea gel and visualized by autoradiography. Core particle formation (third panel) and expression of GFP, as a transfection control (bottom panel), were determined as described in the legends to Fig. 3B and Fig. 2B, respectively. (B) Relative levels of encapsidated pgRNA, compared after normalization to the intracellular RNA level. Data represent means and SD of results from three independent experiments. Statistical significance was evaluated using Student's *t* test. *P* values for differences relative to the STSSSS (WT) protein are indicated by asterisks: *, $P < 0.05$; and **, $P < 0.00005$. Comparisons between the alanine- and glutamate-substituted mutants are indicated by brackets, and the *P* values are shown above the bars. (C) PCR and schematic alignment of splice junctions with ORFs. HBV DNA was extracted from isolated core particles, and PCR was performed to examine the small DNAs shown in Fig. 4A (asterisks). The 2,071-bp full-length HBV DNA and the 814-bp DNA resulting from removal of 1,257 nt from the full-length HBV RNA by splicing were amplified (arrowheads).

first and second panels, lanes 1 versus lanes 8 and 10). This indicates that phosphorylated threonine 162 and either phosphorylated serine 170 or 178 are necessary for efficient pgRNA encapsidation.

Threonine 162 and serines 170 and 178 contribute to HBV DNA synthesis. Next, we used Southern blotting to analyze HBV DNA synthesis in cotransfected Huh7 cells (Fig. 6D). Due to impaired encapsidation by the T162A/S170A, T162A/S178A, and RRR-3A mutants (Fig. 6C, lanes 8, 10, and 14), these mutants exhibited very low levels of HBV DNA synthesis (Fig. 6D, lanes 8, 10, and 14). Consistent with the data in Fig. 4A and B, lanes 5, the RRR-3E mutant exhibited significantly reduced levels of HBV

DNA, and it lacked RC DNA altogether (Fig. 6D, lane 15). All double-alanine- or double-glutamate-substituted mutants exhibited significantly reduced levels of HBV DNA and lacked RC DNA (Fig. 6D, lanes 8 to 13). Consistent with the data in Fig. 4, more dramatic reductions in HBV DNA levels were observed in alanine-substituted mutants than in glutamate-substituted mutants (Fig. 6D). We also immunoprecipitated core particles from lysates of cotransfected cells by using anti-HBc antibody, and then we performed Southern blotting on the immunoprecipitated material (data not shown). This experiment yielded results similar to those shown in Fig. 6D, further confirming that core particles formed by mutant C proteins are efficiently recognized by anti-HBc antibody
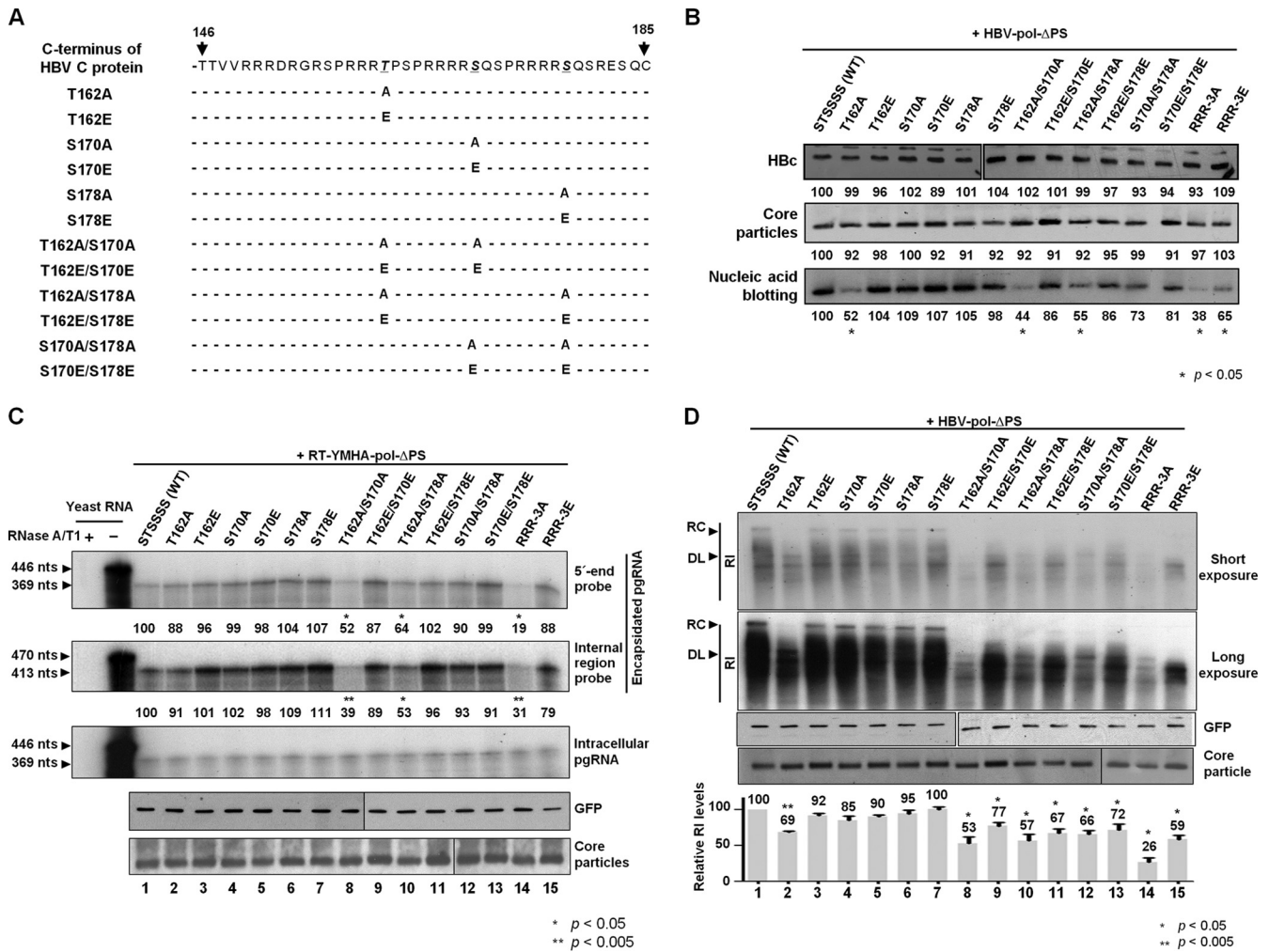
FIG 6 HBV C protein expression, core particle formation, pgRNA encapsidation, and HBV DNA synthesis by mutant C proteins. (A) Amino acid sequences of the C-terminal regions of the STSSSS (WT) protein and single and double mutants of C protein. Threonine 162 and serines 170 and 178 were replaced with alanine(s) or glutamate(s) in various combinations. (B) C proteins, core particles, and nucleic acid blotting from core particles containing STSSSS (WT) or mutant C proteins. C proteins (top panel) and core particles (second panel) were detected as described for Fig. 2B and Fig. 3B, respectively. (Bottom panel) Nucleic acid blotting. After core particle Western blotting, the PVDF membrane was treated with 0.2 N NaOH to expose nucleic acids from the core particles, hybridized with a random-primed ^{32}P-labeled HBV-specific probe, and subjected to autoradiography as described for Southern blotting in the legend to Fig. 4A. (C) RPA was conducted as described for Fig. 5A. For the internal region probe, 470 nt of the HBV sequence was synthesized *in vitro*, and the protected pgRNA (413 nt), representing nt 1262 to 1674 of the HBV sequence, was visualized by autoradiography. Relative levels of encapsidated pgRNAs, obtained using the 5′-end probe (369 nt) and the internal region probe (413 nt), are shown as numbers (expressed as percentages of the level in the STSSSS [WT] strain) below the corresponding gel lanes. Transfection experiments were repeated three times. (D) HBV DNA was extracted from cytoplasmic core particles and analyzed by Southern blotting as described for Fig. 4A. Relative levels of total RI DNAs, including RC and DL DNAs, are shown in the column graph in the bottom panel. Data represent means and SD of results from three independent experiments, and statistical significance was evaluated by Student's *t* test. *P* values for differences relative to the STSSSS (WT) protein are indicated by asterisks: *, $P < 0.05$; and **, $P < 0.005$.

and that overall DNA levels are not affected by micrococcal nuclease treatment (data not shown). The T162A mutant was the only singly substituted mutant to exhibit significantly reduced levels of HBV DNA and to lack RC DNA (Fig. 6D, lane 2 versus lanes 3 to 7), demonstrating that phosphorylated threonine 162 is important for HBV DNA synthesis. Likewise, the S157A, S164A, and S172A single-alanine-substituted mutants (equivalent to the S155A, S162A, and S170A mutants of the ayw subtype) also lacked RC DNA (11), suggesting that, individually, the phosphoacceptor serines 170 and 178 are less critical for HBV DNA synthesis.

To examine the T162A mutant further, we triply transfected Huh7 cells with the STSSSS (WT) and T162A proteins and pHBV-

pol-ΔPS. HBV DNA synthesis was inhibited by increasing amounts of the T162A mutant, whereas pgRNA encapsidation was not altered (data not shown). This result indicates that the T162A mutant exerts a dominant negative phenotype, similar to several previously described serine mutants in SPRRR motifs (22).

Threonine 162 contributes to minus- and plus-strand DNA synthesis and circularization. The stages of HBV DNA replication have been well documented (Fig. 7A) (6, 11, 29–31). In brief, minus-strand DNA synthesis is initiated within the bulge of the stem-loop in the 5′-end epsilon (ε) sequence of pgRNA in P-protein-containing core particles (26, 32). After the P protein is covalently linked to TGAA or GAA (the nascent minus-strand oli-
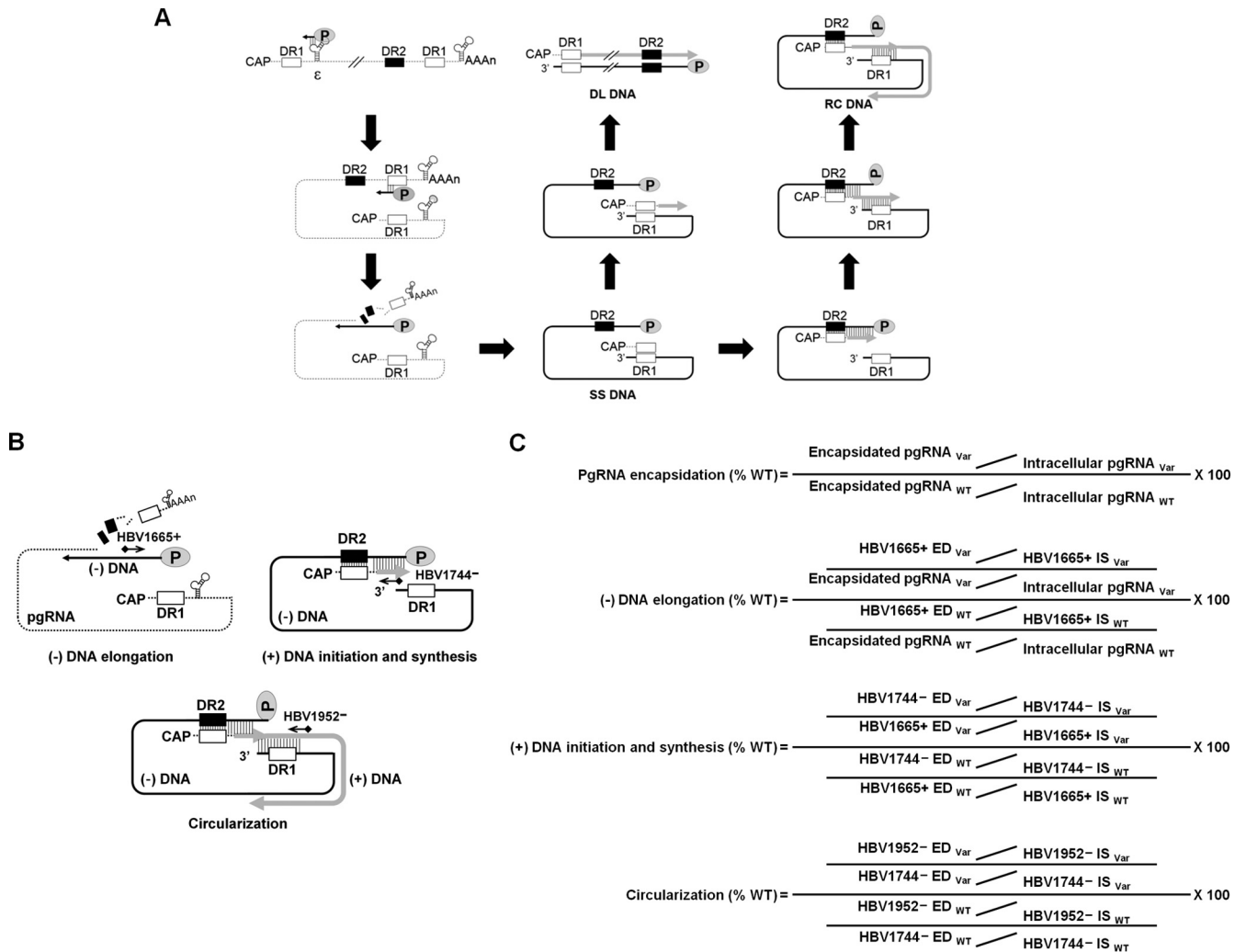
FIG 7 HBV DNA synthesis from pgRNA, and strategies for measuring minus- and plus-strand and circularized DNAs by primer extension analysis. (A) HBV DNA synthesis pathways. pgRNA, the template for minus-strand DNA, has an 11-nt direct repeat (DR1) sequence at the 5′ and 3′ ends (white), as well as another direct repeat (DR2) sequence (black). P protein is associated with the 5′-end epsilon (ε) structure. Minus-strand DNA synthesis is initiated at the epsilon (ε) stem-loop structure of pgRNA, which covalently attaches to P protein as a nascent oligomer. The minus-strand DNA oligomer-linked P protein translocates to the 3′-end DR1 region of pgRNA to elongate minus-strand DNA (minus-strand DNA elongation). RNase H activity of the P protein degrades the pgRNA template to the 5′ end, leaving an uncleaved sequence of about 17 nt that serves as a primer for plus-strand DNA synthesis. When the uncleaved RNA starts to initiate DNA synthesis by *in situ* priming, DL DNA is synthesized. To generate RC DNA, this RNA primer translocates from DR1 to an acceptor site, DR2 of the 5′-end minus-strand DNA template. Plus-strand DNA is synthesized to the 5′ end of the minus-strand DNA template (plus-strand DNA initiation and synthesis). The P protein then switches templates, from the 5′ end to the 3′ end (circularization). Plus-strand DNA is elongated to generate RC DNA. (B) Schematic representation of oligonucleotides used for primer extension analysis. Minus- and plus-strand DNA elongation and circularization were detected using ^{32}P-end-labeled HBV1665+, HBV1744−, and HBV1952−, respectively. (C) Equations used to calculate minus-strand DNA elongation, plus-strand DNA initiation and synthesis, and circularization were adapted from the work of Lewellyn et al. (6, 11), with minor modifications.

gomer) through a hydroxyl bond on tyrosine 65 in the TP domain, it switches templates, moving to the acceptor sequence on direct repeat 1 (DR1) of the 3′ end of pgRNA, and then resumes minus-strand DNA elongation (26, 33, 34). The RNase H domain in the P protein degrades the pgRNA template up to the small fragment at the 5′ end of pgRNA (~17 nt) during minus-strand DNA elongation. This RNA fragment serves as a primer for plus-strand DNA synthesis. When plus-strand DNA elongates at this DR1 position, a process termed *in situ* priming, DL DNAs are synthesized. After the RNA primer translocates to DR2, the 5′ end of the complementary minus-strand template, the plus-strand DNA is synthesized up to the 5′ end of the template. At that point, circularization

occurs through a third template switch to synthesize RC DNA (Fig. 7A).

We performed primer extension analysis by a previously described method (6, 11), with minor modifications, to determine which steps of DNA synthesis (i.e., minus- and plus-strand DNA synthesis and circularization of RC DNA) are affected by phosphoacceptor site mutations in C protein. In these experiments, we used several specific oligonucleotide primers: HBV1665+ to detect the extended minus-strand DNA (Fig. 7B), HBV1744− to measure the plus-strand DNA initiated at DR2 (Fig. 7B), and HBV1952− to detect the circularized DNA (Fig. 7B). For quantitation, the level of extended DNA (ED) was normalized to the level
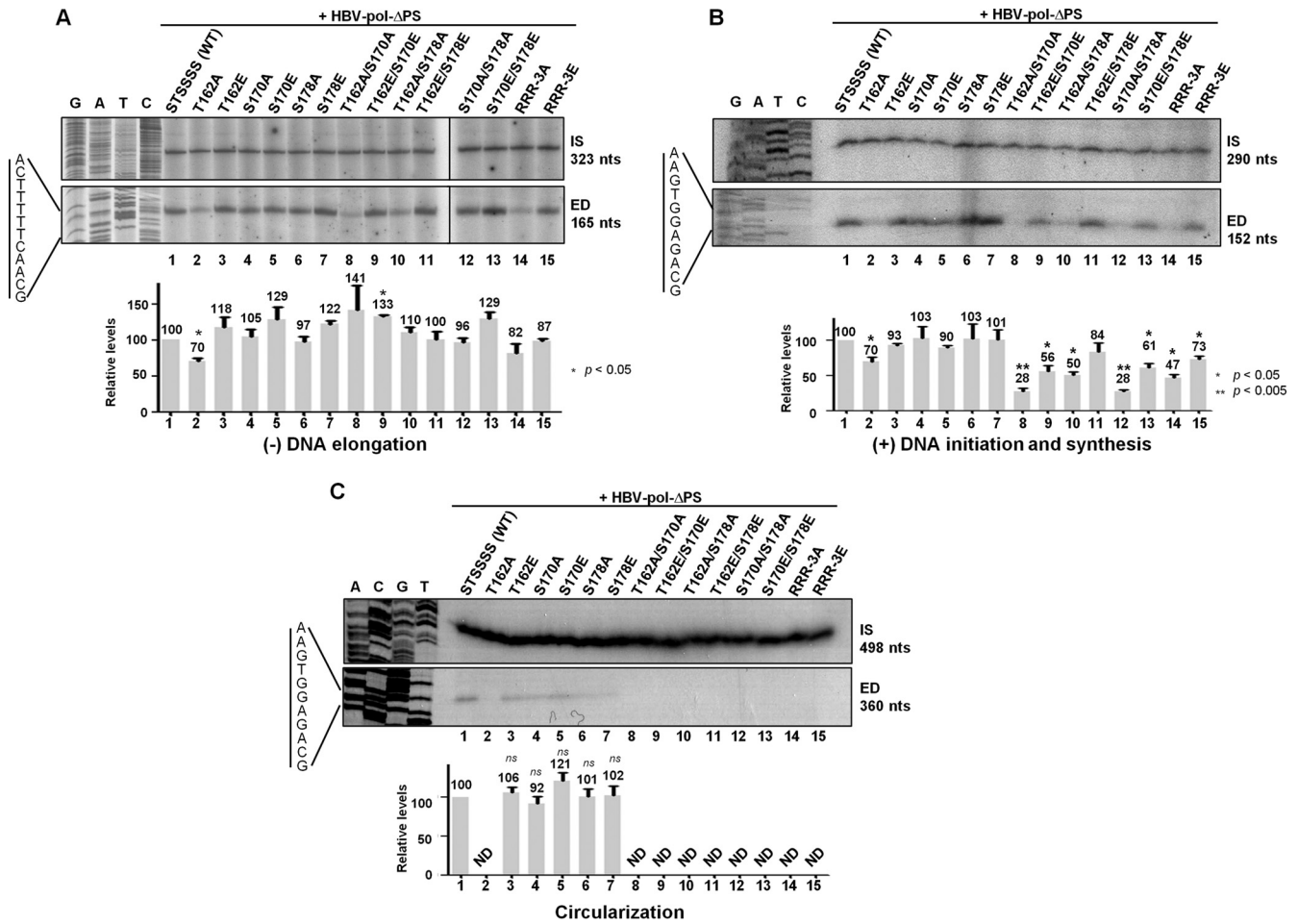
FIG 8 Primer extension analysis to analyze minus-strand DNA elongation, plus-strand DNA initiation and synthesis, and circularization during HBV DNA synthesis. (A) ^{32}P-end-labeled oligonucleotide HBV1665+ was used to detect both the IS and minus-strand DNA that had undergone the template switch to DR1. A sequencing ladder is shown as a reference. The IS was used to normalize and compare the levels of minus-strand DNA elongation. The ED and IS were 165 and 323 nt long, respectively. (B) Primer extension with ^{32}P-end-labeled HBV1744− to detect plus-strand DNA initiation and synthesis. The ED and IS were 152 and 290 nt long, respectively. (C) Primer extension using ^{32}P-end-labeled HBV1952− to detect circularization. The ED and IS were 360 and 498 nt long, respectively. T162A and double- and triple-substitution mutants could not be analyzed because the DNA levels were below the reliable detection level (ND). Histograms show the efficiencies of minus-strand DNA elongation, plus-strand DNA initiation and synthesis, and circularization relative to those with the STSSSS (WT) protein, calculated using the equations shown in Fig. 7C. Data represent means and SD of results from three independent experiments. Statistical significance was evaluated using Student's t test. P values for differences relative to the STSSSS (WT) protein are indicated by asterisks: *, $P < 0.05$; and **, $P < 0.005$.

of a single IS DNA. The levels of extended minus-strand DNA (165 bases), plus-strand DNA at DR2 (152 bases), and circularized DNA (360 bases) were calculated as described by Lewellyn et al. (6, 11), with minor modifications (Fig. 7C). One important feature of these formulas is that a given step is normalized to the output of the previous step, allowing estimation of the efficiency of each step independent of the efficiencies of earlier steps.

The T162A mutant was the only C protein mutant to exhibit reduced minus-strand DNA elongation (70%) (Fig. 8A, lanes 2; Table 1). In contrast, the T162E/S170E mutant exhibited significantly elevated minus-strand DNA elongation (Fig. 8A, lanes 9; Table 1). The T162A mutant and all of the double and triple mutants, except the T162E/178E mutant, exhibited reduced efficiencies of plus-strand DNA initiation and synthesis (Fig. 8B, lanes 2, 8 to 10, and 12 to 15 versus lane 11; Table 1). In general, alanine-substituted mutants exhibited significantly less plus-strand DNA ini-

tiation and synthesis than the corresponding glutamate-substituted mutants, as also observed by Southern blotting (Fig. 4 and 6D).

We then measured the production of RC DNA, the last step in DNA synthesis, by Southern blotting (Fig. 6D; Table 1). When RC DNAs were not detected in cells expressing mutant C proteins, we speculated that the mutants might have defects in circularization (Fig. 6D, lanes 2 and 8 to 15; Table 1). As expected, we could not quantitate the circularized DNA from any of these mutants, because the intensities were too low (Fig. 8C).

The T162A mutant was the only single mutant to exhibit defects in multiple steps of HBV DNA synthesis (i.e., minus- and plus-strand DNA synthesis and circularization of DNA), further demonstrating that threonine 162 contributes to multiple aspects of HBV replication, with the notable exception of pgRNA encapsidation (Fig. 6C and D and Fig. 8, lane 2; Table 1). Most double and triple mutants also exhibited defects at multiple steps of HBV

TABLE 1 Core particle formation, pgRNA encapsidation, minus- and plus-strand DNA elongation, and circularization by STSSSS (WT) and phosphoacceptor site mutant C proteins

Phosphorylation mutant	% of WT level[a]					
	Core particle formation	pgRNA encapsidation	Minus-strand DNA elongation	Plus-strand DNA elongation	Circularization	RC DNA
STSSSS (WT)	100	100	100	100	100	100
T162A	92	91	70	70	ND	ND
T162E	98	101	118	93	106	98
S170A	100	102	105	103	92	88
S170E	92	98	129	90	121	102
S178A	91	109	97	103	101	97
S178E	92	111	122	101	102	105
T162A/S170A	92	39	141	28	ND	ND
T162E/S170E	91	89	133	56	ND	ND
T162A/S178A	92	53	110	50	ND	ND
T162E/S178E	95	96	100	84	ND	ND
S170A/S178A	99	93	96	28	ND	ND
S170E/S178E	91	91	129	61	ND	ND
RRR-3A	97	31	82	47	ND	ND
RRR-3E	103	79	87	73	ND	ND

[a] ND, not determined.

replication, in this case including pgRNA encapsidation. Together, our results demonstrate that the phosphorylation and dephosphorylation of phosphoacceptor residues threonine 162 and serines 170 and 178 within the carboxyl terminus of C protein make multiple contributions to HBV replication.

DISCUSSION

The C proteins of HBV and related hepadnaviruses contain several conserved consensus phosphorylation recognition motifs at their carboxyl termini: SPRRR, S/TP, RS, SR, RxxS/T, and RRRS/T (or RRxS/T). Many of these motifs overlap. The presence of threonine 162, at RRRT (or RRxT), RxxT, and TP sites, and serines 170 and 178, at RRRS (or RRxS), RxxS, and RS sites, suggests that various cellular kinases phosphorylate the C protein with different efficiencies or preferences. (i) The RRxS/T site may be phosphorylated by PKA, cyclic GMP (cGMP)-dependent protein kinase, and p90 ribosomal S6 kinase; the RxxS/T site by protein kinase B (Akt), mitogen- and stress-activated kinase 1/2, and AMP-activated protein kinase; the R/KRxS/T site by p21-activated kinases; and so on. (ii) The S/TP motif may be phosphorylated by proline-directed serine/threonine kinases, such as p34[cdc2] (CDK1) (12), CDK2 (16), and Erk1. (iii) The RS motif among preferred consensus RS and SR dipeptide, RSR, RSP, SPRY, and SRSR phosphorylation sites for SRPK1/2 may be phosphorylated by SRPK1/2 (15).

HBV C protein can be heavily phosphorylated, if necessary, at seven phosphoacceptor sites in the carboxyl terminus. As noted above, these sites are present within overlapping consensus recognition motifs. Therefore, various intracellular kinases may phosphorylate C protein, depending on signaling activation, intracellular localization, and/or cell cycle stage, thereby contributing to temporal and spatial control of HBV replication. The presence of many overlapping consensus phosphorylation sites (Fig. 1) and our results demonstrating weaker effects of glutamate-substituted mutants on HBV replication (Fig. 4, 5, 6, and 8) further strengthen the hypothesis of Lewellyn and Loeb (11) that carboxyl-terminally phosphorylated C protein is more active. Thus, the presence of seven phosphoacceptor sites ensures the availability of active C protein for HBV replication.

Based on the phosphorylation efficiencies of STSSSS (WT) and mutant C proteins, none of the six confirmed phosphoacceptor sites are fully phosphorylated at any given time (Fig. 2B, C, and E), suggesting that a dynamic phosphorylation-dephosphorylation cycle contributes to HBV replication. In the duck HBV (DHBV) C protein, dephosphorylation is important for core particle envelopment and secretion (23); therefore, it is conceivable that dephosphorylation of C protein plays a role in HBV maturation.

Previous studies suggested that positive charges inside core particles are important for genome replication because they cancel the negative charges of encapsidated RNAs. Furthermore, dephosphorylation may be necessary to establish proper charge balance and may therefore be required for completion of genome replication (23, 35, 36). However, consistent with the work of Lewellyn and Loeb (11), our study indicates that dephosphorylation is not required for completion of the plus-strand DNA genome, because dephosphorylation-mimetic alanine-substituted mutants were more defective in genome replication than phosphorylation-mimetic glutamate-substituted mutants (Fig. 4, 5, 6, and 8). Alanine- and glutamate-substituted mutants have fixed charges; therefore, we cannot exclude the possibility that dynamically regulated positive and negative charges are important for replication. Based on the results of ³²Pᵢ labeling experiments, we concluded that C proteins are usually partially phosphorylated and therefore have extra phosphoacceptor residues available for further modification (Fig. 2).

DHBV C proteins from secreted virions are hypophosphorylated (23), and infecting and recycling HBV core particles with RC DNA genomes can enter the nucleus to undergo transcription and amplification of covalently closed circular DNA. Therefore, it is conceivable that mature RC DNA-containing core particles are hypophosphorylated or dephosphorylated and can therefore enter the nucleus. Consistent with this idea, Liao and Ou (8) demonstrated that C proteins containing alanine substitution mutations at SPRRR motifs are mostly localized in the nucleus. We observed that the alanine-substituted 3A-PRRR, RRR-3A, and AAAAAA mutants exhibited severe replication defects, possibly because immature mutant core particles formed by alanine-sub-

stituted mutant C proteins enter the nucleus prematurely. However, we cannot explain the nuclear localization of glutamate-substituted mutants, which also entered the nucleus relatively early: when we examined the nuclear localization of core particles by confocal microscopy, all the triple-alanine- and triple-glutamate-substituted mutant core particles were localized in the nucleus, even 6 h after transfection (data not shown).

Threonine 162 had long been ignored as a phosphoacceptor site, possibly due to the lack of *in vitro* labeling at this position by CK2-activated PKA (18), the notion that PKA may not be the major kinase responsible for phosphorylation of C protein and incorporation into core particles (15), and the lack of recognition and phosphorylation at this position by SRPK1/2 and PKC. However, based on a recent study showing that CDK2 is the major kinase that phosphorylates S/TP sites in the carboxyl termini of hepadnaviral C proteins and is incorporated into core particles (16), it seemed likely that threonine 162 was a *bona fide* phosphoacceptor site. Here we showed for the first time that threonine 162 is indeed phosphorylated in the cell (Fig. 2B, C, and E, lanes 2), although the identity of the responsible kinase remains unknown. Further study will be necessary to determine which kinase phosphorylates threonine 162 and serines 170 and 178 of C protein.

Several lines of evidence converge to indicate that threonine 162 is important for HBV replication: (i) this residue is conserved among mammalian hepadnavirus C proteins (Fig. 1); (ii) this residue is phosphorylated in cells (Fig. 2); (iii) the dephosphorylation-mimetic T162A mutant exerts a dominant negative phenotype (data not shown); and (iv) the T162A mutant causes multiple defects in HBV replication, whereas the phosphorylation-mimetic T162E mutant causes none (Fig. 6 and 8; Table 1; data not shown).

We also investigated whether threonine 162 could be replaced by serine. Phosphorylation levels were comparable between the SSSSSS mutant and STSSSS (WT) C proteins (Fig. 2B, lane 1 versus lane 8, and E, lane 1 versus lane 4 and lane 2 versus lane 5). However, HBV DNA synthesis was slightly reduced in the SSSSSS mutant relative to the STSSSS (WT) strain and in the ESEEEE mutant relative to the ETEEEE mutant (data not shown). This suggests that threonine 162 is replaceable with serine but that threonine is preferable for efficient replication.

Synthesis of DNA smaller than the DL DNA from spliced RNA was previously observed in carboxyl-terminal-deletion C protein mutants, the 3E-PRRR mutant of C protein, or chimeric C protein variants substituted with corresponding residues from the DHBV C protein (3–5). Here we showed that DNAs synthesized from the RRR-3E and EEEEEE mutants were mostly produced from spliced RNA (Fig. 5C), as in the 3E-PRRR mutant. Our Southern blot analyses also indicated that these DNAs were synthesized from spliced RNA (Fig. 4A and 6D). In accordance with previous reports (4, 5), we could not detect a significant bias toward encapsidation of the full-length or spliced RNA in either the STSSSS (WT) strain or the RRR-3E mutant, as determined using the 5′-end and internal region probes (Fig. 5A and 6C; data not shown). Therefore, we speculate that the RRR-3E mutant may have a more serious defect in full-length DNA synthesis than in full-length pgRNA encapsidation, as in the cases of the previously reported carboxyl-terminally deleted mutants and the 3E-PRRR mutant (4, 5). It is possible that the full-length encapsidated pgRNA in the RRR-3E mutant may be nuclease sensitive, resulting in a defect in full-length DNA synthesis, as in the cases of the previously reported mutants (5). Because the RRR-3E mutant exhibits reduced

efficiency in plus-strand DNA synthesis and is defective in circularization and RC DNA synthesis (Fig. 8B and C and Table 1), we hypothesize that the small DNA synthesized from spliced RNA may not have enough space for the second and third template switches, especially the third switch.

Previous work demonstrated that the most important phosphorylated serine at an SPRRR motif (i.e., among serines 157, 164, and 172) is serine 164 (serine 162 in the ayw subtype) (7, 11, 22). Likewise, threonine 162 is the most important phosphorylated residue for HBV replication among residues at an RRRS/T motif (i.e., threonine 162 and serines 170 and 178). These two residues are in very close proximity; therefore, the location itself may be important. Our previous study compared the replications of the HDHD chimeric C variant, whose carboxyl terminus is mostly derived from the DHBV C protein but contains the [167]RRR-SQSPRR[175] motif of the HBV C protein, and the HHDH chimeric C variant, which is mostly derived from the HBV C protein but contains nine DHBV residues ([167]RAGSPLPRS[175]) (3). The HDHD C variant replicated quite well with RC DNA, whereas the HHDH C variant replicated poorly and lacked RC DNA (3). The HDHD C variant contains DHBV-derived threonine 164 at the RxxT and TP motifs, with more than seven putative phosphorylation sites (3), further suggesting that either threonine 162 or threonine 164 in the RxxT and TP motifs and at least seven phosphorylation sites at the carboxyl terminus are required for efficient encapsidation and HBV replication.

ACKNOWLEDGMENTS

REFERENCES

1. **Ganem D, Schneider RJ.** 2001. Hepadnaviridae, p 2923–2969. *In* Knipe DM, Howley PM, Griffin DE, Lamb RA, Martin MA, Roizman B, Straus SE (ed), Fields virology, 4th ed. Lippincott Williams & Wilkins, Philadelphia, PA.
2. **Gallina A, Bonelli F, Zentilin L, Rindi G, Muttini M, Milanesi G.** 1989. A recombinant hepatitis B core antigen polypeptide with the protamine-like domain deleted self-assembles into capsid particles but fails to bind nucleic acids. J. Virol. **63:**4645–4652.
3. **Jung J, Kim HY, Kim TY, Shin BH, Park GS, Park S, Chwae YJ, Shin HJ, Kim K.** 2012. C-terminal substitution of HBV core proteins with those from DHBV reveals that arginine-rich [167]RRRSQSPRR[175] domain is critical for HBV replication. PLoS One **7:**e41087. http://dx.doi.org/10.1371/journal.pone.0041087.
4. **Kock J, Nassal M, Deres K, Blum HE, von Weizsacker F.** 2004. Hepatitis B virus nucleocapsids formed by carboxy-terminally mutated core proteins contain spliced viral genomes but lack full-size DNA. J. Virol. **78:**13812–13818. http://dx.doi.org/10.1128/JVI.78.24.13812-13818.2004.
5. **Le Pogam S, Chua PK, Newman M, Shih C.** 2005. Exposure of RNA templates and encapsidation of spliced viral RNA are influenced by the arginine-rich domain of human hepatitis B virus core antigen (HBcAg 165–173). J. Virol. **79:**1871–1887. http://dx.doi.org/10.1128/JVI.79.3.1871-1887.2005.
6. **Lewellyn EB, Loeb DD.** 2011. The arginine clusters of the carboxy-terminal domain of the core protein of hepatitis B virus make pleiotropic contributions to genome replication. J. Virol. **85:**1298–1309. http://dx.doi.org/10.1128/JVI.01957-10.
7. **Lan YT, Li J, Liao W, Ou J.** 1999. Roles of the three major phosphorylation sites of hepatitis B virus core protein in viral replication. Virology **259:**342–348. http://dx.doi.org/10.1006/viro.1999.9798.
8. **Liao W, Ou JH.** 1995. Phosphorylation and nuclear localization of the hepatitis B virus core protein: significance of serine in the three repeated SPRRR motifs. J. Virol. **69:**1025–1029.

9. **Machida A, Ohnuma H, Tsuda F, Yoshikawa A, Hoshi Y, Tanaka T, Kishimoto S, Akahane Y, Miyakawa Y, Mayumi M.** 1991. Phosphorylation in the carboxyl-terminal domain of the capsid protein of hepatitis B virus: evaluation with a monoclonal antibody. J. Virol. **65:**6024–6030.

10. **Yeh CT, Ou JH.** 1991. Phosphorylation of hepatitis B virus precore and core proteins. J. Virol. **65:**2327–2331.

11. **Lewellyn EB, Loeb DD.** 2011. Serine phosphoacceptor sites within the core protein of hepatitis B virus contribute to genome replication pleiotropically. PLoS One **6:**e17202. http://dx.doi.org/10.1371/journal.pone.0017202.

12. **Yeh CT, Wong SW, Fung YK, Ou JH.** 1993. Cell cycle regulation of nuclear localization of hepatitis B virus core protein. Proc. Natl. Acad. Sci. U. S. A. **90:**6459–6463. http://dx.doi.org/10.1073/pnas.90.14.6459.

13. **Kann M, Gerlich WH.** 1994. Effect of core protein phosphorylation by protein kinase C on encapsidation of RNA within core particles of hepatitis B virus. J. Virol. **68:**7993–8000.

14. **Kau JH, Ting LP.** 1998. Phosphorylation of the core protein of hepatitis B virus by a 46-kilodalton serine kinase. J. Virol. **72:**3796–3803.

15. **Daub H, Blencke S, Habenberger P, Kurtenbach A, Dennemoser J, Wissing J, Ullrich A, Cotton M.** 2002. Identification of SRPK1 and SRPK2 as the major cellular protein kinases phosphorylating hepatitis B virus core protein. J. Virol. **76:**8124–8137. http://dx.doi.org/10.1128/JVI.76.16.8124-8137.2002.

16. **Ludgate L, Ning X, Nguyen DH, Adam C, Mentzer L, Hu J.** 2012. Cyclin-dependent kinase 2 phosphorylates S/T-P sites in the hepadnavirus core protein C-terminal domain and is incorporated into viral capsids. J. Virol. **86:**12237–12250. http://dx.doi.org/10.1128/JVI.01218-12.

17. **Chen C, Wang JC, Zlotnick A.** 2011. A kinase chaperones hepatitis B virus capsid assembly and captures capsid dynamics in vitro. PLoS Pathog. **7:**e1002388. http://dx.doi.org/10.1371/journal.ppat.1002388.

18. **Enomoto M, Sawano Y, Kosuge S, Yamano Y, Kuroki K, Ohtsuki K.** 2006. High phosphorylation of HBV core protein by two alpha-type CK2-activated cAMP-dependent protein kinases in vitro. FEBS Lett. **580:**894–899. http://dx.doi.org/10.1016/j.febslet.2006.01.011.

19. **Kang H, Yu J, Jung G.** 2008. Phosphorylation of hepatitis B virus core C-terminally truncated protein (Cp149) by PKC increases capsid assembly and stability. Biochem. J. **416:**47–54. http://dx.doi.org/10.1042/BJ20080724.

20. **Kang HY, Lee S, Park SG, Yu J, Kim Y, Jung G.** 2006. Phosphorylation of hepatitis B virus Cp at Ser87 facilitates core assembly. Biochem. J. **398:**311–317. http://dx.doi.org/10.1042/BJ20060347.

21. **Gazina EV, Fielding JE, Lin B, Anderson DA.** 2000. Core protein phosphorylation modulates pregenomic RNA encapsidation to different extents in human and duck hepatitis B viruses. J. Virol. **74:**4721–4728. http://dx.doi.org/10.1128/JVI.74.10.4721-4728.2000.

22. **Melegari M, Wolf SK, Schneider RJ.** 2005. Hepatitis B virus DNA replication is coordinated by core protein serine phosphorylation and HBx expression. J. Virol. **79:**9810–9820. http://dx.doi.org/10.1128/JVI.79.15.9810-9820.2005.

23. **Perlman DH, Berg EA, O'Connor BP, Costello CE, Hu J.** 2005. Reverse

transcription-associated dephosphorylation of hepadnavirus nucleocapsids. Proc. Natl. Acad. Sci. U. S. A. **102:**9020–9025. http://dx.doi.org/10.1073/pnas.0502138102.

24. **Kann M, Sodeik B, Vlachou A, Gerlich WH, Helenius A.** 1999. Phosphorylation-dependent binding of hepatitis B virus core particles to the nuclear pore complex. J. Cell Biol. **145:**45–55. http://dx.doi.org/10.1083/jcb.145.1.45.

25. **Wittkop L, Schwarz A, Cassany A, Grun-Bernhard S, Delaleau M, Rabe B, Cazenave C, Gerlich W, Glebe D, Kann M.** 2010. Inhibition of protein kinase C phosphorylation of hepatitis B virus capsids inhibits virion formation and causes intracellular capsid accumulation. Cell. Microbiol. **12:**962–975. http://dx.doi.org/10.1111/j.1462-5822.2010.01444.x.

26. **Kim HY, Park GS, Kim EG, Kang SH, Shin HJ, Park S, Kim KH.** 2004. Oligomer synthesis by priming deficient polymerase in hepatitis B virus core particle. Virology **322:**22–30. http://dx.doi.org/10.1016/j.virol.2004.01.009.

27. **Park GS, Kim HY, Shin HS, Park S, Shin HS, Kim K.** 2008. Modulation of hepatitis B virus replication by expression of polymerase-surface fusion protein through splicing: implications for viral persistence. Virus Res. **136:**166–174. http://dx.doi.org/10.1016/j.virusres.2008.05.005.

28. **Ko CK, Shin Y-C, Park W-J, Kim S, Kim J, Ryu W-S.** 2014. Residues Arg703, Asp777, and Arg781 of the RNase H domain of hepatitis B virus polymerase are critical for viral DNA synthesis. J. Virol. **88:**154–163. http://dx.doi.org/10.1128/JVI.01916-13.

29. **Lewellyn EB, Loeb DD.** 2007. Base pairing between cis-acting sequences contributes to template switching during plus-strand DNA synthesis in human hepatitis B virus. J. Virol. **81:**6207–6215. http://dx.doi.org/10.1128/JVI.00210-07.

30. **Nassal M.** 2008. Hepatitis B viruses: reverse transcription a different way. Virus Res. **134:**235–249. http://dx.doi.org/10.1016/j.virusres.2007.12.024.

31. **Wang GH, Seeger C.** 1993. Novel mechanism for reverse transcription in hepatitis B viruses. J. Virol. **67:**6507–6512.

32. **Tavis JE, Perrl S, Ganem D.** 1994. Hepadnavirus reverse transcription initiates within the stem-loop of the RNA packaging signal and employs a novel strand transfer. J. Virol. **68:**3536–3543.

33. **Nassal M, Rieger A.** 1996. A bulged region of the hepatitis B virus RNA encapsidation contains the replication origin for discontinuous first-strand DNA synthesis. J. Virol. **70:**2764–2773.

34. **Rieger A, Nassal M.** 1996. Specific hepatitis B virus minus-strand DNA synthesis requires only the 5-encapsidation signal and the 3-proximal direct repeat DR1. J. Virol. **70:**585–589.

35. **Schlicht HJ, Bartenschlager R, Schaller H.** 1989. The duck hepatitis B virus core protein contains a highly phosphorylated C terminus that is essential for replication but not for RNA packaging. J. Virol. **63:**2995–3000.

36. **Basagoudanavar SH, Perlman DH, Hu J.** 2007. Regulation of hepadnavirus reverse transcription by dynamic nucleocapsid phosphorylation. J. Virol. **81:**1641–1649. http://dx.doi.org/10.1128/JVI.01671-06.